

Landscape Influences on Ecosystem Function: Local and Routing Control of Oxygen Dynamics in a Floodplain Aquifer

H. Maurice Valett,^{1,3*} F. Richard Hauer,^{1,2,3} and Jack A. Stanford^{1,2,3}

¹Division of Biological Sciences, University of Montana, Missoula, Montana 59812, USA; ²Flathead Lake Biological Station, University of Montana, 32125 Bio Station Lane, Polson, Montana 59860, USA; ³Montana Institute on Ecosystems, University of Montana, Missoula, Montana, USA

ABSTRACT

Perspectives addressing either “local” or “routing” control over ecological form and function alternatively emphasize ambient conditions or recognize that form and processes at one location may be heavily influenced by other points in space. In their natural state, floodplains of montane gravel-bed rivers are organized laterally into parafluvial zones, where scour occurs annually, and orthofluvial environments, within which active (that is, early successional) and passive (that is, late successional) zones differ in regard to flooding influences. Vertically, these rivers interact with extensive alluvial aquifers throughout the length of their floodplains. We addressed how local and routing controls organize riverscape structure and function by investigating seasonal dynamics of interstitial dissolved oxygen (DO) vertically within the alluvial aquifer, longitudinally along flowpaths, and laterally across active and passive orthofluvial (PO) zones in the Nyack floodplain, Middle Fork Flat-

head River, MT. Groundwater DO was positively correlated to pH and negatively correlated electrical conductivity (EC) across all seasons. In some wells (7 of 19), DO was significantly lower and EC greater at shallow depths, and the magnitudes of vertical zonation were related to dissolved organic carbon concentrations. Longitudinal declines in DO were always and exclusively observed along flowpaths of the PO zone. At the same time, persistent hypoxic patches within the active orthofluvial environment suggest metabolic hotspots that contribute to local control of physicochemistry. In ecosystems heavily influenced by material transport, local and routing controls may be manifested simultaneously as distinct patterns of organization, which are expressed at different spatial and temporal scales.

Key words: floodplain; aquifer; flowpath; oxygen.

Received 25 January 2013; accepted 9 August 2013;
published online 3 December 2013

Electronic supplementary material: The online version of this article (doi:10.1007/s10021-013-9717-5) contains supplementary material, which is available to authorized users.

Author Contributions: HMV conducted analysis of the data and wrote the paper with input from FRH and JAS. FRH and JAS designed the original study and supervised collection of the original data.

*Corresponding author; e-mail: maury.valett@umontana.edu

INTRODUCTION

A great deal of ecological theory has centered on how local conditions influence ecological structure and function. Local habitat heterogeneity may lead to different community composition (Hutchinson 1961), invasion potential (Levine 2000), or vital rates (Dimond and Armstrong 2007). Theories of

ecological succession in plant communities have emphasized endogenous (that is, local) processes as drivers of community change (Connell and Slatyer 1977). In desert landscapes, “islands of fertility” (Schlesinger and others 1996) emphasize how plant patches influence local ecosystem structure (for example, soil moisture, nitrogen content).

At the same time, ecological form and function at one location may be heavily influenced by linkage to other points in space (Turner 1989). Metapopulation theory (Hanski 1998) and its outgrowth to metacommunities (Leibold and others 2004) and metaecosystems (Loreau and others 2003) similarly emphasize movement and connectivity. Recent focus on spatial subsidies to food webs (Polis and others 2004) and the long-standing recognition of the importance of allochthonous inputs for aquatic ecosystems including marshes (Odum and de La Cruz 1963), streams (Minshall 1967; Fisher and Likens 1973; Mulholland and others 1985), lakes (Jansson and others 2000; Pace and others 2004), and estuaries (Howarth and others 1996; Hopkinson and others 1998) illustrate the importance of material transport in determining ecological structure and function at multiple levels of ecological organization.

Montgomery (1999) succinctly described these different perspectives as emphasizing either “local” or “routing” control. In this sense, ecosystems may be perceived to contain a mosaic of patches or, alternatively, to be composed of a linked series of interacting subsystems. There is no doubt that both local and routing forces influence all ecological systems to some degree (for example, Ricklefs 1987). However, understanding circumstances under which one or the other form of “control” is dominant will help guide heuristic and mechanistic models addressing structure and function at multiple levels of ecological organization.

In their natural state, floodplains of montane gravel-bed rivers are a mosaic of biophysical patches (Stanford and others 2005) that form as an interplay among flooding, sediment transport, and change as a result of successional response by riparian vegetation (Whited and others 2007). Floodplains are also extensions of the river system with zones of interaction defined by the character of flow and mass transport (Figure 1A). The river’s main and side channels are surrounded by the “parafluvial zone,” floodplain surfaces denuded of vegetation by scour during floods (Stanford and others 2005). The “ortho-fluvial zone” is less frequently flooded, but still regularly inundated. Deposition of fine sediments in the ortho-fluvial zone contributes to soil building processes associ-

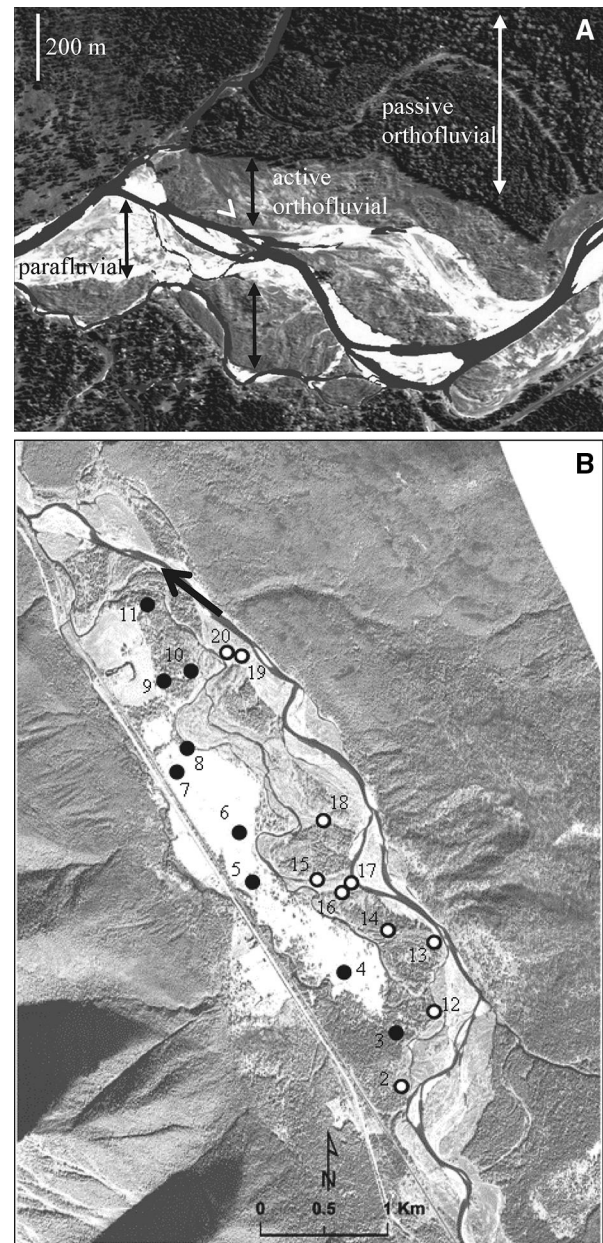


Figure 1. **A** Biophysical zones of montane riverscapes. **B** Monitoring well locations on the Nyack floodplain, Middle Fork Flathead River, MT (main channel and flow direction are indicated by black arrow). Wells are established along transects occupying the passive (*filled symbols*) and active (*open symbols*) ortho-fluvial floodplain zones. Due to its placement on a tributary terrace, well #1 (not shown) was excluded from assessment. Knick points delineating the start and end of the floodplain are outside of the scope of the map.

ated with seral stages of riparian vegetation (Whited and others 2007). Within the ortho-fluvial environment, surfaces vary from early stages of riparian succession with poorly developed soils that

are rapidly aggrading [that is, active orthofluvial (AO) zone] to those occupied by old growth stands of mixed forests characterized by more organic-rich soils [that is, passive orthofluvial (PO)] that are then eventually destroyed by large infrequent floods or locally removed as the result of channel avulsion (Whited and others 2007).

Floodplains of gravel-bed rivers house alluvial aquifers (that is, hyporheic zones) that may extend for kilometers laterally from the main river channel (Stanford and Ward 1988) as surface water from the river feeds the subsurface through sediments of highly variable composition and hydraulic character. Flowpaths within the alluvial aquifer have residence times that may vary from hours to months or years (Helton and others 2012) and serve as habitat for groundwater microbes (Ellis and others 1998; Pusch and others 1998) and metazoans (Stanford and Ward 1988). Accordingly, these vast hyporheic zones are metabolically active (Craft and others 2002), support biogeochemical processes that transform and remove nutrients and carbon (Stanford and others 2005), and affect algal (Wyatt and others 2008) and macroinvertebrate (Pepin and Hauer 2002) growth and composition at sites of return flow. Understanding controls over subsurface processes is complicated by heterogeneity in alluvial composition (Helton and others 2012) and flowpath complexity (Poole 2002), along with temporal variation at the scale of storms, seasonal change, and climate cycles (Harvey and Bencala 1993; Heffernan and others 2008).

In this paper, we apply local and routing perspectives to interpret ecosystem form and function for the alluvial aquifer of the Nyack floodplain, Middle Fork Flathead River. Flowing water ecosystems in general, and river floodplain landscapes in particular, are model systems for this sort of investigation because they are characterized by both advective fluxes of water (Fisher and others 2004) and concomitant hierarchical structuring of habitat patches (Pringle and others 1988). Here, we investigate how interstitial dissolved oxygen (DO) dynamics are organized through space and time vertically within the alluvial aquifer, longitudinally by flowpaths, and laterally across the active and PO floodplain zones. To do this, we rely on an extensive network of wells established over decades of research on this sentinel study site. Using basic measures of water composition, we address how spatial organization and biotic activity are reflected in DO patterns to describe how alluvial aquifer ecosystems are alternatively organized by flowpath routing or local conditions characteristic of floodplain landscapes.

METHODS

Study Site

The study was conducted in the Nyack floodplain, Middle Fork Flathead River, MT, USA, characterized by a snowmelt-driven hydrograph with the flood pulse occurring in late spring and early summer (Appendix A in supplementary material). The floodplain (975 m elevation) is 10 km long and averages 1.5 km width. River water enters the floodplain through an upstream bedrock constriction (that is, knick point) and forms anastomosed channels that exchange water with the aquifer throughout the floodplain. The alluvial aquifer is an extensive hyporheic zone that consists of coarse heterogeneous sediments ranging in size from clay to boulders with a diverse subsurface microbial and metazoan food web (Stanford and Ward 1988; Ellis and others 1998). Groundwater flow within the aquifer is predominantly horizontal (Diehl 2004) and gradual thinning of alluvial material towards downstream portions of the floodplain that ends in confining bedrock is primarily responsible for return flows to spring brooks, back-waters, and the river's main channel

Well Grid Design and Installation

The sampling network on the Nyack floodplain consists of 57 groundwater wells and seven surface water sampling locations. Deep wells (6.35–12.45 m maximum depth below ground) were installed with a motorized hollow-stem auger, slotted (2.04–2.55 mm openings) throughout their length, and were used to assess vertical and longitudinal aquifer physicochemical structure over seasonal and annual time scales. Deep wells were located along one of two transects oriented roughly parallel to the river along the length of the floodplain (Figure 1B). Wells were assigned to AO and PO zones based on field recognizance and disturbance mapping provided by Whited and others (2007). An additional 37 shallow wells (5.1 cm diameter; 3–5 m maximum depth below ground) were installed using a hydraulic GeoprobeTM. Shallow wells were slotted from 1 to 3 m depth and were used along with shallow portions of deep wells to generate spatially explicit, floodplain-wide maps of aquifer DO. Sampling locations were recorded using GPS and GIS facilities (ESRI 2010) and transverse (distance from the main channel) and longitudinal (distance down the floodplain relative to a datum established at the upstream knick point) distances determined for all sites.

Floodplain stratigraphy and aquifer hydraulic conductivity were assessed during well installation

for all deep wells as documented by Diehl (2004). Stratigraphy was investigated and documented by examining and interpreting well logs, by analysis of split spoon samples of bore holes at various points, and by cross-referencing these observations with resistance to drilling. Notes available from well installation (Diehl 2004) detailed ease of drilling with depth and when combined with the other sources of information provided distinction among soil, silt/clay, sand, gravel, and cobble layers for deep monitoring wells. Depth-discrete hydraulic conductivity (K , md^{-1}) was estimated using pneumatic slug tests for partially penetrating wells in highly conductive formations as specifically described by Butler and others (2003). Discrete K estimates were made at intervals using a double-packer systems where screened sections within the well were isolated by o-rings and inflatable rubber packers used to restrict slug tests to 1-m intervals over various well depths.

Ground Water and Surface Water Sampling

Physicochemical conditions (see below) were monitored seasonally using field probes from November 2003 to June 2005 (Appendix A in supplementary material) including all surface sites, shallow groundwater flowpaths (that is, 1 m depth below water table in all wells), and vertical profiles in deep wells during baseflow, ascending, and descending limbs of the flood pulse. Surveys of deep wells that included vertically discrete sampling occurred during all seasons in 2004 and again in spring 2005 (Appendix A in supplementary material). Samples collected during spring 2004 and 2005 were combined for seasonal comparisons. Samples for dissolved organic carbon (DOC) were collected from the full suite of deep wells ($n = 19$) in summer and autumn and from fewer wells in winter ($n = 5$) and spring ($n = 6$). Some wells were repeatedly sampled during summer and autumn (Reid 2007) and individual samples were used to generate grand means for aquifer physicochemical measures. Average values for a given well and season, however, were used during analyses of seasonal variation to avoid inflated sample sizes.

Sample water was drawn from the wells at a rate of 12 L/min using a 12 V DC electric submersible pump (Whale Submersible 881, Whale Systems Specialists; Bangor, Ireland) at rates that ensured short residence times in sampling chambers and accurate portrayal of aquifer conditions (Reid 2007). DO (mg/L, %sat), temperature ($^{\circ}\text{C}$), electrical conductivity (EC as specific conductance,

$\mu\text{S cm}^{-1}$), and pH were recorded using YSI 550A or YSI 55 (Yellow Springs, Inc., Yellow Spring, WI) or automated sondes (Hydrolab Surveyor 4a, Hydrolab Hach Hydromet, Loveland, CO). A foam straddle packer isolated 0.5-m sampling intervals in deep wells and the uppermost 1 m of all wells during shallow surveys. Before taking readings, water was purged for at least 3 min prior to sampling to clear ~ 15 resident volumes.

Samples for DOC were collected and filtered in the field (Whatman GFF, 0.7 μm pore size) into glass bottles, placed on ice, and returned to the laboratory, where they were preserved by freezing if not analyzed immediately upon return. DOC concentrations were measured via high temperature combustion on a Tekmar-Dohrmann Apollo 9000HS carbon analyzer (Teledyne Tekmar, Mason, OH, USA).

Oxygen Contouring

We used the inverse distance weighted kriging algorithm in ArcMapTM 10 (ESRI 2010) to interpolate the spatial distribution of DO across the floodplain as derived from deep and shallow ($n = 57$) monitoring wells. An initial interpolation was created at a 50-m resolution and then isopleths were derived at increments of 1 mg/L. Using these isopleths, the final DO distribution map was created at a 10-m resolution to smooth out boundaries.

Statistical Assessment

All statistical assessment comparing spatial and temporal differences in river and aquifer physicochemistry was done using SAS software (SAS Institute, Cary, NC). We used parametric correlations (Pearson product-moment) to address physicochemical variables using single values to represent each well annually and seasonally for the floodplain as whole ($n = 19$) and for active ($n = 10$) and passive ($n = 9$) orthofluvial zones. The same approach was used to address relationships between K and physicochemical composition among and within wells. Temporal change in ecosystem structure was addressed using one-way ANOVA followed by Tukey's HSD with season as the main effect for both untransformed data and z scores generated from temporal data sets following equation (1) where y_i , \bar{y} , and SD are individual observations, mean values, and standard deviations for a given well, normalizing for spatial variation among wells

$$z \text{ score} = \left(\frac{y_i - \bar{y}}{SD} \right) \quad (1)$$

Longitudinal and transverse locations were used in regression models to address continuous spatial patterns in physicochemical structuring. Vertical profiles of aquifer physicochemistry consistently illustrated inflections at about 5 m depth. Accordingly, we calculated differences between means for shallow (<5 m) and deep (≥ 5 m) zones to assess the extent of vertical zonation for physicochemical measures and hydraulic conductivity for each well and season (paired *t* tests, $n = 5/\text{well}$). We also used differences between annual means ($n = 19$ wells) to address floodplain physicochemical zonation.

RESULTS

River water had greater oxygen content (10.3 ± 1.3 mg/L DO; $86.1 \pm 7.5\%$ saturation), lower EC (159 ± 33 $\mu\text{S cm}^{-1}$), and higher pH (8.1 ± 0.4) than did groundwater (grand mean \pm SE; Table 1). River temperature ($7.8 \pm 4.3^\circ\text{C}$) was alternatively greater than and less than observed for individual wells. Average DO in the alluvial aquifer was as low as 1.5 ± 0.8 mg/L (12.1 \pm 6.4%) and as high as 8.4 ± 2.5 mg/L (69.0 \pm 14.3%). Groundwater EC was 2–129 $\mu\text{S cm}^{-1}$ greater, and pH 0.01–0.81 U less, than in the river (Table 1).

Patterns in Physicochemical Conditions

Temperature and DO content of groundwater changed while EC and pH remained unaltered across seasons on the Nyack floodplain (Table 2). Groundwater DO concentrations in winter and spring were 50.0 and 46.1% of saturation, respectively, and significantly greater (Table 2, $P < 0.05$, ANOVA, Tukey's HSD on *z* scores) than concentrations during summer (34.8%) and autumn (37.9%). Water temperatures were lower ($P < 0.05$, ANOVA *z* scores) during winter and spring (5.2 and 6.1°C) compared to summer and autumn (9.4 and 8.2°C). By contrast, despite significant differences in *z*pH values among seasons ($P = 0.0087$, Table 2), mean pH varied by only 0.05 U. Average EC ranged only 5.5–7.2 $\mu\text{S cm}^{-1}$ across seasons and did not differ significantly as absolute ($P = 0.9728$) or *z* scores ($P = 0.3145$). The same patterns were evident in AO wells with DO and temperature displaying seasonal variation and a general lack of variation in pH and conductivity (Table 2). In the PO zone, average seasonal values for DO (both absolute and % saturation) were lower than mean values in the AO zone, except during summer when DO in wells of the AO zone averaged 0.5 mg/L (4.3% sat) less than in the PO zone. Across

Table 1. Physicochemical Conditions in the Middle Fork Flathead River, AO, and PO Environments

Well	Zone	n	Dissolved oxygen (mg/L)	Dissolved oxygen (% sat)	Temperature ($^\circ\text{C}$)	EC ($\mu\text{S cm}^{-1}$)	pH	Dissolved organic carbon (mg/L)
River	River	35–82	10.3 ± 1.3	86.1 ± 7.5	7.8 ± 4.3	159 ± 33	8.10 ± 0.4	0.81 ± 0.41 (82)
AO2	Active	27	8.4 ± 2.5	69.0 ± 14.3	8.2 ± 5.1	161 ± 21	7.89 ± 0.16	0.57 ± 0.07 (4)
AO12	Active	50	3.8 ± 2.4	29.8 ± 17.5	6.7 ± 3.6	271 ± 89	7.29 ± 0.18	0.66 ± 0.22 (8)
AO13	Active	52	6.3 ± 1.8	50.7 ± 11.7	6.7 ± 2.7	203 ± 12	7.95 ± 0.11	0.29 ± 0.05 (4)
AO14	Active	40	7.6 ± 1.3	61.8 ± 8.4	6.5 ± 2.1	183 ± 8	8.09 ± 0.12	0.86 ± 1.07 (4)
AO15	Active	25	5.0 ± 1.0	41.4 ± 7.1	7.0 ± 1.1	219 ± 25	7.98 ± 0.09	0.40 ± 0.39 (67)
AO16	Active	30	5.4 ± 1.2	44.7 ± 9.8	7.5 ± 2.0	228 ± 49	7.89 ± 0.25	0.48 ± 0.09 (6)
AO17	Active	37	3.1 ± 2.1	25.7 ± 17.0	7.3 ± 2.3	270 ± 55	7.57 ± 0.21	0.77 ± 0.40 (8)
AO18	Active	35	7.0 ± 1.8	57.6 ± 11.3	7.9 ± 3.1	183 ± 21	8.00 ± 0.13	0.60 ± 0.53 (4)
AO19	Active	28	3.9 ± 2.1	28.6 ± 19.0	7.6 ± 1.2	243 ± 23	7.79 ± 0.11	0.46 ± 0.36 (4)
AO20	Active	31	3.0 ± 1.4	24.6 ± 11.1	8.3 ± 2.5	256 ± 16	7.79 ± 0.08	0.71 ± 0.94 (4)
PO3	Passive	31	7.9 ± 2.1	62.5 ± 12.9	6.2 ± 3.4	191 ± 11	7.64 ± 0.15	0.37 ± 0.06 (4)
PO4	Passive	54	7.4 ± 1.9	60.6 ± 15.1	7.0 ± 1.5	210 ± 25	7.89 ± 0.37	0.72 ± 0.41 (4)
PO5	Passive	54	6.3 ± 0.5	51.5 ± 4.5	6.5 ± 1.3	221 ± 16	7.92 ± 0.06	0.29 ± 0.10 (4)
PO6	Passive	28	6.3 ± 0.6	51.1 ± 4.0	6.3 ± 0.6	228 ± 22	7.96 ± 0.06	0.27 ± 0.04 (4)
PO7	Passive	38	5.5 ± 0.6	44.4 ± 4.6	6.3 ± 0.8	248 ± 30	7.85 ± 0.14	0.27 ± 0.07 (4)
PO8	Passive	23	4.0 ± 0.3	33.5 ± 2.9	7.6 ± 0.8	259 ± 11	7.69 ± 0.20	0.26 ± 0.03 (4)
PO9	Passive	13	4.1 ± 0.3	34.0 ± 1.8	6.9 ± 1.3	244 ± 6	7.88 ± 0.05	0.27 ± 0.03 (4)
PO10	Passive	25	1.5 ± 0.8	12.1 ± 6.4	7.3 ± 2.1	261 ± 13	7.67 ± 0.13	0.46 ± 0.18 (20)
PO11	Passive	28	2.5 ± 0.9	20.5 ± 7.2	7.3 ± 1.6	288 ± 21	7.46 ± 0.13	0.74 ± 0.86 (4)
Wells	All	649	5.5 ± 2.6	44.5 ± 19.8	7.0 ± 2.5	226 ± 49	7.8 ± 0.27	0.50 ± 0.50 (173)

Data are grand mean \pm standard deviation where $n =$ total number of observations for a given well including replicate samples within wells and across sampling dates. EC = specific electrical conductivity. Values in parentheses are total numbers of observations for DOC.

seasons, groundwater of the PO zone was cooler during summer and autumn, comparable during spring, and warmer during winter when compared to groundwater of the AO zone (Table 2). In general, however, seasonal change in the PO zone was muted. Absolute concentrations of DO differed among seasons ($P = 0.0467$), but no two seasonal means differed significantly from each other (Table 2). When measured as % saturation, DO did not differ with season ($P = 0.0643$). Finally, although zPH differed significantly among seasons ($P = 0.0020$), the seasonal range in mean pH for PO wells was less than 0.1 U.

Except for a positive correlation with EC in the PO zone, temperature was generally not related to other physicochemical variables ($P > 0.05$). However, on three occasions DO (% saturation) and temperature were significantly and negatively correlated (Table 3), with the strongest relationship displayed among wells of the PO zone at the annual time scale ($r = -0.72$, $P = 0.0282$) and during summer ($r = -0.71$, $P = 0.0312$). By contrast, measures of DO (% saturation), EC, and pH were tightly related across all wells at annual and seasonal time scales (Table 3). Declining DO was associated with lower pH ($r = 0.60$, $P = 0.0065$)

Table 2. Seasonal Comparison of Groundwater Physicochemical Conditions in the Nyack Floodplain, Middle Fork Flathead River

Zone	P	Autumn	Winter	Spring	Summer
All wells					
Dissolved oxygen (DO, mg/L)	0.0087	4.50 ^{AB} (19)	6.40 ^A (17)	5.80 ^{AB} (17)	4.04 ^B (19)
Dissolved oxygen (% saturation)	0.0492	37.9 ^A (19)	50.0 ^A (17)	46.1 ^A (17)	34.8 ^A (19)
Temperature (°C)	<0.0001	8.2 ^A (19)	5.2 ^B (17)	6.1 ^B (17)	9.4 ^A (19)
EC (µS cm ⁻¹)	0.9728	231.8 (19)	226.3 (17)	228.5 (17)	227.5 (19)
pH	0.8883	7.77 (19)	7.79 (17)	7.82 (17)	7.78 (19)
zDO	<0.0001	-0.35 ^B (19)	0.88 ^A (17)	0.61 ^A (17)	-0.44 ^B (19)
z%sat	<0.0001	-0.43 ^B (19)	0.61 ^A (17)	0.28 ^A (17)	-0.57 ^B (19)
ztemp	<0.0001	0.63 ^A (19)	-0.85 ^B (17)	-0.46 ^B (17)	0.99 ^A (19)
zcond	0.3145	0.24 (19)	-0.06 (17)	-0.08 (17)	-0.07 (19)
zPH	0.0087	-0.32 ^B (19)	-0.12 ^A (17)	0.39 ^A (17)	-0.14 ^B (19)
Active orthofluvial					
Dissolved oxygen (DO, mg/L)	0.0075	5.00 ^{AB} (10)	7.40 ^A (10)	6.19 ^{AB} (9)	3.69 ^B (10)
Dissolved oxygen (% saturation)	0.0339	42.1 ^{AB} (10)	50.0 ^A (10)	48.8 ^{AB} (9)	32.5 ^B (10)
Temperature (°C)	<0.0001	8.4 ^{AB} (10)	4.8 ^C (10)	6.4 ^{BC} (9)	10.0 ^A (10)
EC (µS cm ⁻¹)	0.9942	218.2 (10)	219.7 (10)	214.2 (9)	217.1 (10)
pH	0.9992	7.81 (10)	7.82 (10)	7.82 (9)	7.81 (10)
zDO	<0.0001	-0.35 ^B (10)	1.02 ^A (10)	0.23 ^B (9)	-1.03 ^C (10)
z%sat	<0.0001	-0.23 ^B (10)	0.99 ^A (10)	0.16 ^B (9)	-0.99 ^C (10)
ztemp	<0.0001	0.64 ^A (10)	-0.96 ^B (10)	-0.42 ^B (9)	0.97 ^A (10)
zcond	0.3156	0.19 (10)	0.20 (10)	-0.30 (9)	0.02 (10)
zPH	0.4262	-0.16 (10)	0.07 (10)	0.25 (9)	-0.28 (10)
Passive orthofluvial					
Dissolved oxygen (DO, mg/L)	0.0467	4.05 ^A (9)	5.40 ^A (7)	5.46 ^A (8)	4.36 ^A (9)
Dissolved oxygen (% saturation)	0.0643	34.0 (9)	42.7 (7)	43.6 (8)	36.8 (9)
Temperature (°C)	<0.0001	7.9 ^A (9)	5.6 ^B (7)	6.0 ^B (8)	8.8 ^A (9)
EC (µS cm ⁻¹)	0.868	244.0 (9)	232.9 (7)	241.3 (8)	236.8 (9)
pH	0.698	7.73 (9)	7.75 (7)	7.82 (8)	7.76 (9)
zDO	0.0488	-0.44 ^A (9)	0.75 ^A (7)	0.94 ^A (8)	0.05 ^A (9)
z%sat	0.0275	-0.61 ^B (9)	0.22 ^{AB} (7)	0.39 ^A (8)	-0.19 ^B (9)
ztemp	<0.0001	0.62 ^A (9)	-0.72 ^B (7)	-0.50 ^B (8)	1.00 ^A (9)
zcond	0.1517	0.29 (9)	-0.32 (7)	0.11 (8)	-0.16 (9)
zPH	0.0020	-0.46 ^B (9)	-0.30 ^B (7)	0.51 ^A (8)	-0.02 ^{AB} (9)

*Each well was represented by a single value derived as the mean of depth-specific measures. Data are means (n) for each season where n = number of wells analyzed per season. P values represent results from one-way ANOVA assessment of differences among seasons. Following significant seasonal effect (that is, $P < 0.05$), means within a row with unique superscripts are significantly different ($\alpha = 0.05$, Tukey's HSD multiple comparison test). EC = specific electrical conductivity.

whereas EC increased with declining DO ($r = -0.91$, $P < 0.0001$). Further, increasing EC was associated with significant decline in pH ($r = -0.69$, $P < 0.001$). These same relationships were evident when active and passive zones were assessed independently either within or across seasons (except for a lack of significant correlation, that is, $P > 0.05$, involving pH in the PO zone, Table 3).

Vertical Zonation of Aquifer Structure

Aquifer stratigraphy varied spatially among wells with heterogeneous distribution of particle sizes predominantly composed of sand, gravel, and cobble (Appendix B in supplementary material). Overlying soil depths ranged from 0 to 2.7 m (average = 1.1 ± 0.2 m, $n = 19$ wells) and depth to water table varied from 0.65 to 3.36 m across wells and seasons (data not shown). Average K varied from a low of 237 m day^{-1} to a high of 530 m day^{-1} (Appendix C in supplementary material). Hydraulic conductivity differed with depth in some wells (for example, PO9, PO4), but other wells were characterized by very little vertical variation

(for example, AO2, AO14) and average values for deep (that is, >5 m) strata were not significantly different from measures made at more shallow depths (paired t test, $P > 0.05$). Variation in hydraulic conductivity was not related to apparent aquifer stratigraphy (Appendix B in supplementary material) and no significant correlations between K and any physicochemical metrics were found within or among any combination of wells.

Depth profiles within wells revealed repeated patterns of vertical physicochemical zonation in the Nyack aquifer. Visual inspection of vertical trends within individual wells (Figure 2) indicated two types of physicochemical profiles: (1) orthograde—little vertical distinction in physicochemical measures, (2) clinograde (cl)—evident physicochemical gradients, with or without vertical differences in temperature. Of 19 deep wells, 12 were classified as orthograde and 7 as cl (Table 4). Five cl wells (AO12, AO13, AO16, AO17, AO18) were located in the AO zone whereas two (PO4, PO5) were found in the PO zone (Table 4).

Shallow and deep strata of cl wells differed significantly ($P < 0.05$, paired t test) in terms of DO, EC, and pH (Table 4). On average DO in shallow

Table 3. Relationships Among Groundwater Physicochemical Conditions in the Nyack Floodplain, Middle Fork Flathead River

Zone	Annual	Autumn	Winter	Spring	Summer
All wells					
EC X DO	-0.91, <0.0001, 19	-0.90, <0.0001, 19	-0.82, <0.0001, 17	-0.85, 0.0001, 17	-0.56, 0.0116, 19
pH X DO	0.60, 0.0065, 19	0.62, 0.0045, 19	0.58, 0.0123, 17	0.53, 0.0266, 17	0.58, 0.0087, 19
Temp X DO	-0.26, 0.2836, 19	-0.24, 0.3183, 19	-0.60, 0.0087, 17	0.09, 0.7357, 17	-0.38, 0.1062, 19
EC X pH	-0.69, <0.001, 19	-0.63, 0.0037, 19	-0.77, 0.0002, 17	-0.67, 0.0032, 17	-0.80, <0.0001, 19
EC X Temp	0.04, 0.8708, 19	0.06, 0.7994, 19	0.28, 0.2573, 17	-0.24, 0.3459, 17	-0.26, 0.2816, 19
pH X Temp	-0.03, 0.9003, 19	-0.18, 0.4527, 19	0.09, 0.7150, 17	0.16, 0.5289, 17	-0.19, 0.4171, 19
Active orthofluvial					
EC X DO	-0.97, <0.0001, 10	-0.96, <0.0001, 10	-0.84, 0.0024, 10	-0.94, <0.0001, 9	-0.74, 0.0145, 10
pH X DO	0.66, 0.035, 10	0.68, 0.0316, 10	0.61, 0.059, 10	0.68, 0.042, 9	0.62, 0.0538, 10
Temp X DO	-0.02, 0.9496, 10	-0.34, 0.3265, 10	-0.54, 0.1061, 10	0.26, 0.4991, 9	-0.13, 0.7131, 10
EC X pH	-0.78, 0.008, 10	-0.77, 0.0085, 10	-0.86, 0.0013, 10	-0.80, 0.0092, 9	-0.19, 0.5802, 10
EC X Temp	-0.09, 0.7946, 10	0.18, 0.6166, 10	0.16, 0.6456, 10	-0.44, 0.2324, 9	-0.25, 0.5017, 10
pH X Temp	0.08, 0.8115, 10	-0.04, 0.9007, 10	0.21, 0.5450, 10	0.11, 0.7707, 9	-0.09, 0.7928, 10
Passive orthofluvial					
EC X DO	-0.89, 0.0012, 9	-0.85, 0.0036, 9	-0.83, 0.0109, 7	-0.85, 0.0069, 8	-0.56, 0.11, 9
pH X DO	0.53, 0.140, 9	0.53, 0.143, 9	0.59, 0.1259, 7	0.37, 0.3370, 8	0.64, 0.060, 9
Temp X DO	-0.72, 0.0282, 9	-0.09, 0.8168, 9	-0.67, 0.0679, 7	-0.17, 0.6671, 8	-0.71, 0.0312, 9
EC X pH	-0.49, 0.178, 9	-0.59, 0.092, 9	-0.86, 0.0052, 7	-0.22, 0.6000, 8	-0.20, 0.580, 9
EC X Temp	0.67, 0.0466, 9	-0.01, 0.9822, 9	0.47, 0.2376, 7	0.43, 0.2843, 8	-0.08, 0.8300, 9
pH X Temp	-0.49, 0.1783, 9	-0.62, 0.0714, 9	-0.14, 0.7420, 7	0.33, 0.4146, 8	-0.63, 0.0651, 9

Bold values indicate statistically significant ($P < 0.05$) relationships.

*Each well was represented by a single value derived as the mean of depth-specific measures.

Comparisons relate average values across all wells ($n = 19$) or for active ($n = 10$) and passive ($n = 9$) floodplain zones. Data are Pearson correlation coefficients (r , P) based on annual or seasonal observations.

EC = specific conductivity ($\mu\text{S cm}^{-1}$) and DO is dissolved oxygen (% saturation).

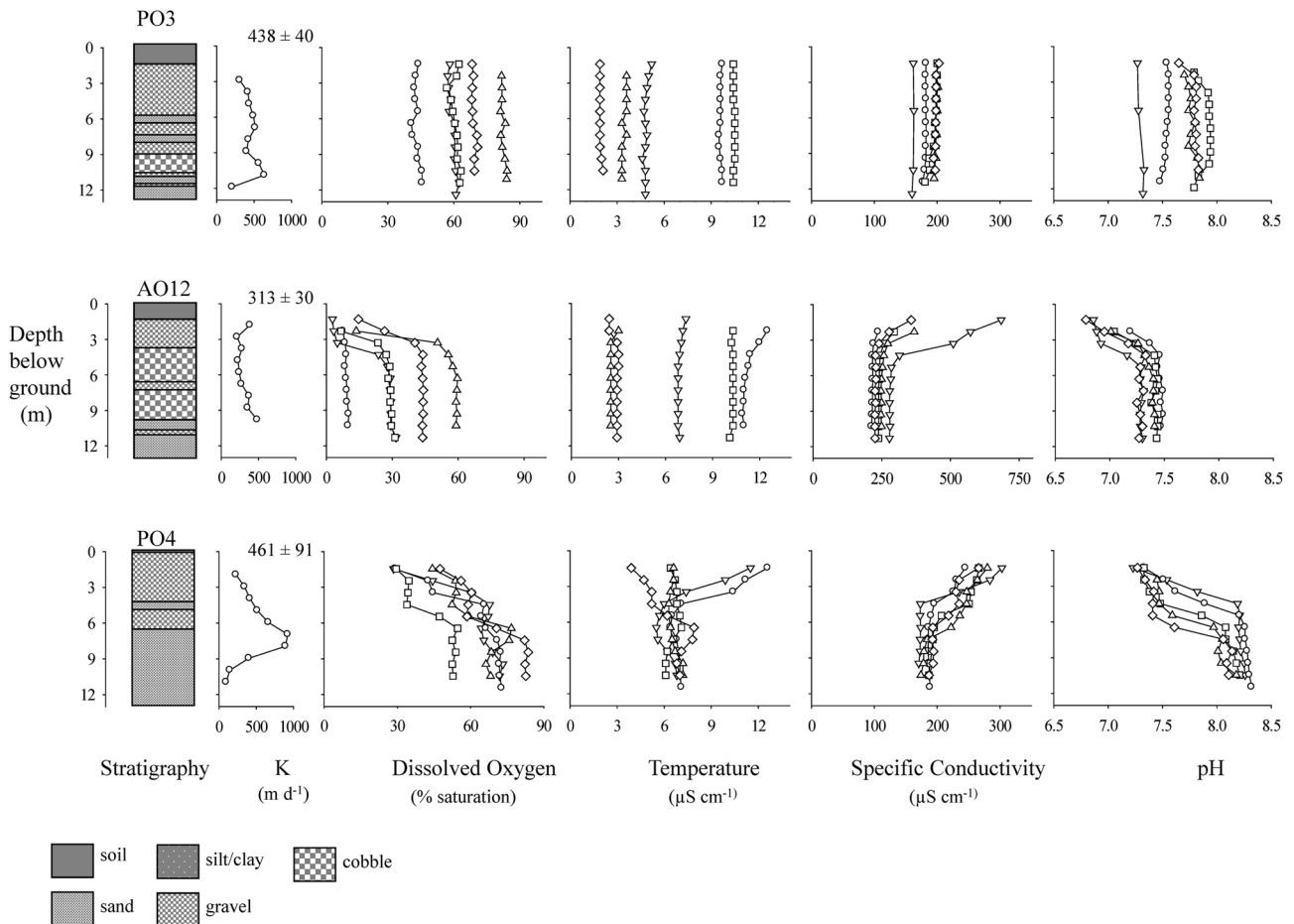


Figure 2. Profiles within wells reveal that vertical zonation of groundwater physicochemistry is not related to aquifer stratigraphy or saturated hydraulic conductivity (K , m day^{-1}). Physicochemical changes with increasing depth below ground illustrate two vertical patterns including: (1) orthograde—generally lacking vertical distinction; and (2) cl—evident and consistent gradients for DO, EC, and pH with or without concomitant thermal zonation. Data are individual measures from wells PO3 (top row), AO12 (middle row), and PO4 (bottom row) taken in June 2004 (inverted triangle), August 2004 (circle), November 2004 (square), January 2005 (triangle), and May 2005 (diamond). Wells names include prefix for active (AO) or passive (PO) orthofluvial zones and numbers that are the same as those provided in Figure 1. Numeric values are average hydraulic conductivity (mean \pm standard error) derived from assessment of discrete measure within each well.

water of cl wells was as much as 3.1–6.2 mg/L (18 to 47.7% sat) lower than in deeper portions of the same wells. Water in shallow depths of cl wells was also of greater ionic strength; on average shallow EC was more than $50 \mu\text{S cm}^{-1}$ greater in four of nine cl wells, and maximum differences revealed by individual vertical profiles ranged from 132.1 to $407 \mu\text{S cm}^{-1}$ (Figure 2; Table 4). In addition to being relatively hypoxic with higher ionic strength, shallow water was between 0.3 and 1.0 pH units more acidic (Table 4).

Across physicochemical variables the magnitudes of vertical differences were quantitatively related in consistent ways suggesting a robust coupling among metrics (Table 5). For all wells and seasons ($n = 73$), the extent of decline in DO was tightly

linked to the magnitude of increase in EC ($r = -0.74$, $P < 0.0001$) and decrease in pH ($r = 0.81$, $P < 0.001$). In addition, decline in pH was correlated to increase in EC ($r = -0.59$, $P < 0.0001$). The direction and magnitude of vertical changes in EC, pH, and DO were even more closely related when wells were segregated by floodplain zone and season (that is, $r = 0.8$ – 0.9 , Table 5).

In contrast to the other measures of physicochemistry, differences in the thermal content of shallow and deep groundwater were less frequently and inconsistently linked to vertical distinctions in DO, EC, or pH (Table 5). In general, annual relationships addressing vertical differences in physicochemistry with differences in temperature were not significant ($P > 0.05$), but differences in

Table 4. Vertical Differences in Groundwater Physicochemical Characteristics for Deep Wells in the AO or PO Zones of the Nyack Floodplain, Middle Fork Flathead River, MT

Well	Zone	Type	Dissolved oxygen (% saturation)			Temperature (°C)			EC ($\mu\text{S cm}^{-1}$)			pH		
			Mean	Max	P	Mean	Max	P	Mean	Max	P	Mean	Max	P
AO2	Active	ortho	0.5	13.4	n.s.	0.1	0.6	n.s.	0.8	4.1	n.s.	0.09	0.48	n.s.
AO12	Active	clino	-12.8	46.0	*	0.4	1.6	n.s.	81.4	407.0	**	-0.21	0.55	*
AO13	Active	clino	-1.9	9.5	*	0.2	1.2	n.s.	14.3	64.6	**	-0.11	0.32	*
AO14	Active	ortho	0.3	3.8	n.s.	0.1	2.3	n.s.	-0.9	10.5	n.s.	0.02	0.20	n.s.
AO15	Active	ortho	-2.5	12.0	n.s.	-0.2	0.9	n.s.	3.4	9.3	n.s.	-0.02	0.34	n.s.
AO16	Active	clino	-8.7	21.1	*	0.0	4.7	n.s.	51.1	117.4	*	-0.28	0.68	*
AH17	Active	clino	-20.1	50.0	**	0.2	8.4	n.s.	74.8	199.0	**	-0.22	0.80	**
AO18	Active	clino	-5.3	42.4	**	0.3	5.9	n.s.	9.1	97.9	*	-0.07	0.43	*
AO19	Active	ortho	0.6	1.9	n.s.	0.0	0.4	n.s.	-0.7	5.0	n.s.	0.04	0.16	n.s.
AO20	Active	ortho	0.2	3.5	n.s.	0.2	2.0	n.s.	-0.7	8.0	n.s.	0.00	0.15	n.s.
PO3	Passive	ortho	-1.1	6.5	n.s.	0.0	0.6	n.s.	3.4	5.0	n.s.	-0.03	0.08	n.s.
PO4	Passive	clino	-20.6	47.7	***	0.7	6.2	n.s.	57.3	132.1	***	-0.61	1.00	***
PO5	Passive	clino	-1.7	9.0	*	0.1	2.5	n.s.	2.9	11.0	***	-0.03	0.20	**
PO6	Passive	ortho	1.2	4.8	n.s.	0.2	1.2	n.s.	-1.8	11.0	n.s.	-0.01	0.10	n.s.
PO7	Passive	ortho	-1.4	11.0	n.s.	0.1	1.0	n.s.	4.1	42.0	n.s.	-0.07	0.53	n.s.
PO8	Passive	ortho	-2.4	6.0	n.s.	0.0	1.7	n.s.	-16.2	37.0	n.s.	-0.21	0.45	*
PO9	Passive	ortho	-1.2	4.8	n.s.	0.0	0.7	n.s.	2.4	6.0	n.s.	-0.02	0.08	n.s.
PO10	Passive	ortho	0.1	15.0	n.s.	-0.4	0.9	n.s.	5.1	29.0	*	-0.06	0.30	n.s.
PO11	Passive	ortho	-1.9	15.1	n.s.	-0.1	1.1	n.s.	7.9	40.0	n.s.	-0.02	0.18	n.s.

*Each stratum was represented by a single value derived as the mean of depth-specific measures for that stratum during each of five seasonal samplings. Wells grouped by zone and types are designated following patterns of vertical stratification of physicochemical variables. Data are annual averages (mean) and maximal single values (max) of differences between shallow (<5 m) and deep (≥ 5 m) strata (that is, shallow—deep). P values reflect results from paired t tests within wells ($n = 5/\text{well}$) to assess differences between strata. Bolded lettering indicates wells with significant vertical zonation.

temperature between deep and shallow strata were related to differences in DO, EC, and pH during both winter and summer (Table 5). However, the same physicochemical differences positively correlated with temperature difference during winter (Δ pH and Δ DO, Table 5) were negatively correlated with temperature differences during the summer. Similarly, differences in EC were negatively correlated to temperature differences in winter, but were positively correlated during summer. These trends were robust across all wells and in the active and PO zones independently.

Longitudinal and Lateral Structure

In addition to displaying distinct vertical zonation, aquifer physicochemical structure was longitudinally related to distance from the floodplain knick point (Figure 3, Appendix C in supplementary material). For the floodplain as a whole, annual DO declined linearly from around 70 to 20% saturation (Figure 3A) whereas EC increased from about 160 to 290 $\mu\text{S cm}^{-1}$ (Figure 3B) such that water lost 1.1 mg/L DO (8.6% saturation) and gained 17 $\mu\text{S cm}^{-1} \text{ km}^{-1}$ along 4,200 m of floodplain flowpath. Along flowpaths of the PO zone (Fig-

ure 3C, D), physicochemical conditions were even more robustly related to longitudinal position; linear models revealed that distance from the floodplain knick point explained 80 and 90% of the variation in DO and EC, respectively (Appendix C in supplementary material). By contrast, groundwater physicochemistry in the AO zone was not organized along flowpaths (Figure 3E, F); regressions against distance from the floodplain knick point were not statistically significant for any variable (Appendix C in supplementary material). Neither temperature nor pH changed predictably with longitudinal distance ($P > 0.05$) based on annual or seasonal means for all wells or for active or PO zones independently (Appendix C in supplementary material).

At the scale of the entire floodplain, organization along flowpaths was evident from autumn through spring, but was lost during summer for all physicochemical variables (Appendix C in supplementary material). Whole-system response resulted from the combined influences of the AO zone, where any measure of physicochemistry was rarely longitudinally organized during any season (Appendix C in supplementary material), and the PO where DO and EC changed significantly ($P < 0.05$) and predictably (R^2 often greater than 0.80 for DO and EC, Appendix

C in supplementary material) along longitudinal flowpaths during all seasons.

This spatial patterning is reflected in response surfaces illustrating seasonal distribution of DO in the alluvial aquifer of the Nyack floodplain (Figure 4). Seasonal decline in DO at the whole floodplain scale is illustrated by the decrease in blue and increase in yellow during winter and spring (Figure 4A, B) and the enhanced red zones of the lower panels during summer and autumn (Figure 4C, D). Focal areas of low DO are evident as red spots, some of which are consistently associated with particular cl (for example, AO12, AO17), or orthograde (PO10, PO11) wells that together represent four of the five lowest mean annual DO concentrations among all orthofluvial wells (Table 1). Continuous transitions from blue to yellow and red along the PO zone are evident for all seasons whereas more patchy and discontinuous coloration depicts the lack of longitudinal organization along the AO zone (Figure 4A–D).

Organic Carbon Influences on Spatial Organization of Aquifer Structure

The average DOC concentration in the Middle Fork of the Flathead River was 0.81 ± 0.05 mg/L ($n = 82$, Table 1) and concentrations during spring (1.22 ± 0.07 mg/L, $n = 6$) were significantly greater ($P < 0.001$) than in summer (0.57 ± 0.05 mg/L, $n = 19$), autumn (0.54 ± 0.05 mg/L, $n = 19$), and winter (0.68 ± 0.06 , $n = 5$) whereas concentrations among those seasons were not significantly different (one-way ANOVA Tukey's test on DOC and zDOC values, data not shown). The annual mean concentration in the river was greater than the mean concentration in all wells except AO14 (0.86 ± 1.07 mg/L, Table 1). Average groundwater DOC concentration was least (0.35 ± 0.03 mg/L, mean \pm SE) during winter and was greatest (0.50 ± 0.06 mg/L) during autumn. Concentrations did not differ significantly among seasons ($P > 0.05$) for absolute DOC or for DOC z scores (data not shown). Groundwater DOC did not vary with longitudinal distance at any spatial scale ($P > 0.05$), but DOC concentration did decline from about 0.75 to 0.25 mg/L with distance from the river channel ($R^2 = 0.33$, $P = 0.010$, Figure 5A). This pattern of decline occurred during summer ($r = -0.53$, $P = 0.017$) and autumn ($r = -0.52$, $P = 0.018$), but not during winter or spring ($P > 0.05$) when fewer wells were sampled. Average temperature, DO, EC, and pH were not related to mean DOC concentration, but DOC content was a strong predictor of the vertical structure of these

physicochemical variables in wells characterized by cl profiles (Figure 5B–D). The intensity of vertical zonation for DO and EC increased significantly with DOC abundance (Figure 5B, C); DOC concentration explained 81 and 57% of the variance in vertical differences for DO and EC, respectively. Vertical stratification of pH was also associated with increasing DOC, but the relationship was not significant ($R^2 = 0.333$, $P = 0.17$, Figure 5D).

DISCUSSION

In open ecosystems understanding changes in the form and abundance of energy and materials requires characterizing both the role of transport into and out of systems and local processes of consumption and production (Odum 1956; Fisher and others 2004). Lacking specific measures of flow at all relevant scales and spatially distributed measures of aquifer metabolism, it is beyond the scope of this research to unequivocally assign the relative importance of these influences on observed patterns of groundwater DO across space and time in the alluvial aquifer of the Nyack floodplain. We contend, however, that assessment of patterns along multiple spatial dimensions (vertical, lateral, and horizontal), through time, and among physicochemical measures, can further understanding of how local and routing control vary in their influence over aquifer form and function.

Longitudinal Organization of Aquifer Structure: Routing Control

With distance down the floodplain, linear declines in DO were accompanied by concomitant increases in EC but little change in temperature (Appendix C in supplementary material). Although not significantly related to distance from the floodplain knickpoint, pH generally declined longitudinally as water chemistry evolved along flowpaths of the Nyack aquifer. During most of the year, this routing control generates a predictable continuum of conditions akin to position within a drainage network that bestows physical and chemical conditions to which biota respond (Vannote and others 1980). This organization is lost during summer when uptake of DO is not linearly organized (Figure 3), physicochemical conditions are discontinuous at the whole floodplain scale, and aquifer heterogeneity reflects variation at smaller, more local spatial scales (Figure 4).

As supported by hydrologic models (Poole and others 2004; Helton and others 2012), wells in the PO zone appear to be linked along flowpaths

Table 5. Differences (Δ) Between Average Values for Shallow (<5 m) and Deep Strata for Physicochemical Measures from Deep Wells of the Nyack Floodplain, Middle Fork Flathead River, MT

Zone	All observations	Autumn	Winter	Spring	Summer
All wells					
Δ EC X Δ DO	-0.74 , <0.0001, 72	-0.79 , <0.0001, 19	-0.83 , <0.0001, 17	-0.79 , 0.0001, 17	-0.84 , <0.0001, 19
Δ pH X Δ DO	0.81 , <0.0001, 72	0.90 , <0.0001, 19	0.73 , 0.0008, 17	0.81 , <0.0001, 17	0.88 , <0.0001, 19
Δ EC X Δ pH	-0.60 , <0.0001, 72	-0.63 , 0.0037, 19	-0.77 , 0.0002, 17	-0.67 , 0.0032, 17	-0.80 , <0.0001, 19
Δ T X Δ pH	-0.25 , 0.0291, 72	-0.08, 0.7335, 19	0.78 , 0.0002, 17	-0.26, 0.3158, 17	-0.88 , <0.0001, 19
Δ T X Δ DO	-0.18, 0.1265, 72	-0.19, 0.4447, 19	0.51 , 0.0331, 17	0.17, 0.5150, 17	-0.86 , <0.0001, 19
Δ T X Δ EC	0.04, 0.7272, 72	0.30, 0.2080, 19	-0.68 , 0.0026, 17	0.05, 0.8470, 17	0.84 , <0.0001, 19
Active orthofluvia					
Δ EC X Δ DO	-0.77 , <0.0001, 39	-0.83 , 0.0030, 10	-0.79 , 0.0059, 10	-0.79 , 0.0106, 9	-0.94 , <0.0001, 10
Δ pH X Δ DO	0.74 , <0.0001, 39	0.93 , <0.0001, 10	0.67 , 0.0322, 10	0.80 , 0.0099, 9	0.82 , 0.0036, 10
Δ EC X Δ pH	-0.72 , <0.0001, 39	-0.88 , 0.0008, 10	-0.92 , 0.0002, 10	-0.76 , 0.0168, 9	-0.91 , 0.0002, 10
Δ T X Δ pH	-0.21, 0.1942, 39	0.33, 0.3466, 10	0.64 , 0.0464, 10	0.34, 0.3621, 9	-0.86 , 0.0013, 10
Δ T X Δ DO	-0.06, 0.7191, 39	0.20, 0.5874, 10	0.24, 0.4869, 10	0.10, 0.7851, 9	-0.86 , 0.0014, 10
Δ T X Δ EC	-0.03, 0.8622, 39	-0.53, 0.1182, 10	-0.67 , 0.0336, 10	0.04, 0.9904, 9	0.87 , 0.0009, 10
Passive orthofluvia					
Δ EC X Δ DO	-0.86 , <0.0001, 33	-0.79 , 0.0102, 9	-0.96 , 0.0004, 7	-0.97 , <0.0001, 8	-0.98 , <0.0001, 9
Δ pH X Δ DO	0.91 , <0.0001, 33	0.98 , <0.0001, 9	0.98 , 0.0001, 7	0.95 , 0.0003, 8	0.94 , 0.0002, 9
Δ EC X Δ pH	-0.81 , <0.0001, 33	-0.72 , 0.0291, 9	-0.97 , 0.0002, 7	-0.98 , <0.0001, 8	-0.93 , 0.0003, 9
Δ T X Δ pH	-0.31, 0.0798, 33	-0.30, 0.4294, 9	0.91 , 0.0048, 7	-0.81 , 0.0137, 8	-0.93 , 0.0003, 9
Δ T X Δ DO	-0.34, 0.0516, 33	-0.37, 0.3317, 9	0.93 , 0.0026, 7	-0.78 , 0.0211, 8	-0.93 , 0.0003, 9
Δ T X Δ EC	0.20, 0.0798, 33	0.72, 0.0299, 9	-0.95 , 0.0012, 7	0.74 , 0.0336, 8	0.93 , 0.0003, 9

Bold values indicate statistically significant ($P < 0.05$) relationships.

*Each stratum was represented by a single value derived as the mean of depth-specific measures for that stratum during each of five seasonal samplings or by the average of those measures for annual assessments.

Data are Pearson correlation coefficients (r , P , n) for all monitoring wells combined and for active and passive floodplain zones based on all or seasonal observations. EC = specific conductivity ($\mu\text{S cm}^{-1}$) and DO is dissolved oxygen (% saturation).

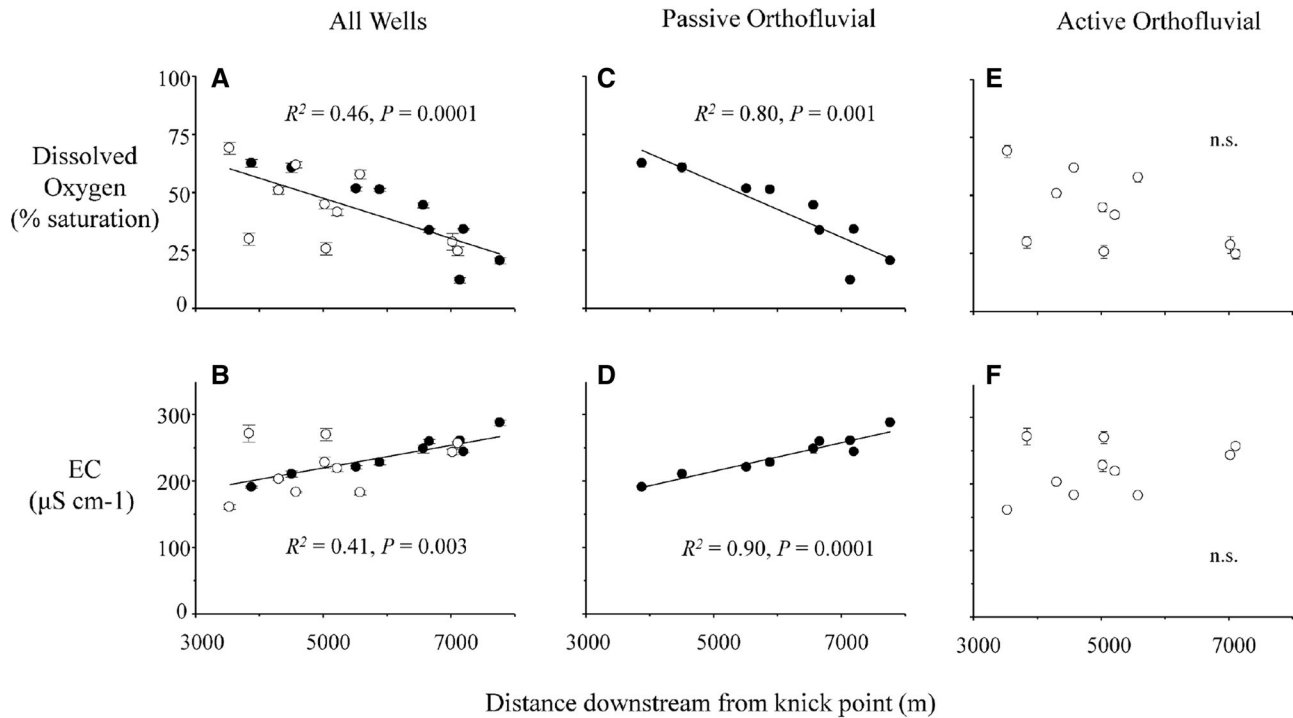


Figure 3. Longitudinal organization of annual average values for DO (% saturation) and EC (specific EC, $\mu\text{S cm}^{-1}$) is evident for the whole floodplain (**A**, **B**) and for the PO zone (**C**, **D**), but is absent among wells of the AO zone (**E**, **F**). Data are mean values ($\pm\text{SE}$, $n = 5$) for individual wells derived by combining seasonal averages.

aligned parallel to the valley's longitudinal axis that remain intact across seasonal changes in physical, chemical, and biological conditions. Smith and others (2011) documented declines in DO for selected wells in the PO zone of the Nyack aquifer similar to those reported here. In their study, DO declined at a rate of $0.002 \text{ mg O}_2/\text{L m}^{-1}$, a value similar to that obtained from our regression of annual means for PO wells ($0.0015 \text{ mg O}_2/\text{L m}^{-1}$, Appendix C in supplementary material). Both these estimates are low compared to those reported by Malard and Hervant (1999) for nine widely distributed, confined groundwater systems ($0.01\text{--}0.09 \text{ mg O}_2 \text{ L}^{-1} \text{ m}^{-1}$) with flowpath lengths between 0.3 and 80 km. Flow paths along the Nyack floodplain are unconfined and longitudinal patterns of gas content are potentially influenced by exchange with the atmosphere. Indeed, work by Smith and others (2011) on the Nyack aquifer documented progressive depletion of $^{18}\text{O}\text{--O}_2$ pools along a PO flowpath of around 3 km length. Microbial respiration along such a flow path should result in enrichment of the residual $^{18}\text{O}\text{--O}_2$ pool and Smith and others (2011) proposed diffusive inputs of diatomic atmospheric oxygen as a causal mechanism for observed patterns of depletion. Thus, to the extent that slopes of DO removal re-

flect net changes in oxygen content, observed declines may underestimate rates of oxygen removal along orthofluvial flowpaths.

Local Influences: Patches, Flowpaths, and Metabolism

Large scale routing control along the channel's longitudinal axis fails to characterize the physico-chemistry of the AO zone at any time scale of assessment; instead the groundwater environment appears as a series of patches with distinct chemical character. This patchwork is illustrated by the mosaic of colors representing groundwater DO in the AO portions of the kriged maps for the alluvial aquifer (Figure 4). The patchy character of the AO zone persists across seasons, but its influence on spatial patterning at the whole floodplain scale is generally overwhelmed by routing control within the PO zone. Only during summer does the patchy character of the AO zone combine with a weakening of longitudinal organization in the PO (Appendix C in supplementary material) to drive loss of routing control at the whole floodplain scale.

Smith and others (2011) reported a decline of $0.06 \text{ mg O}_2 \text{ L}^{-1} \text{ m}^{-1}$ along a 100-m flowpath adjacent to the Middle Fork's main channel, a

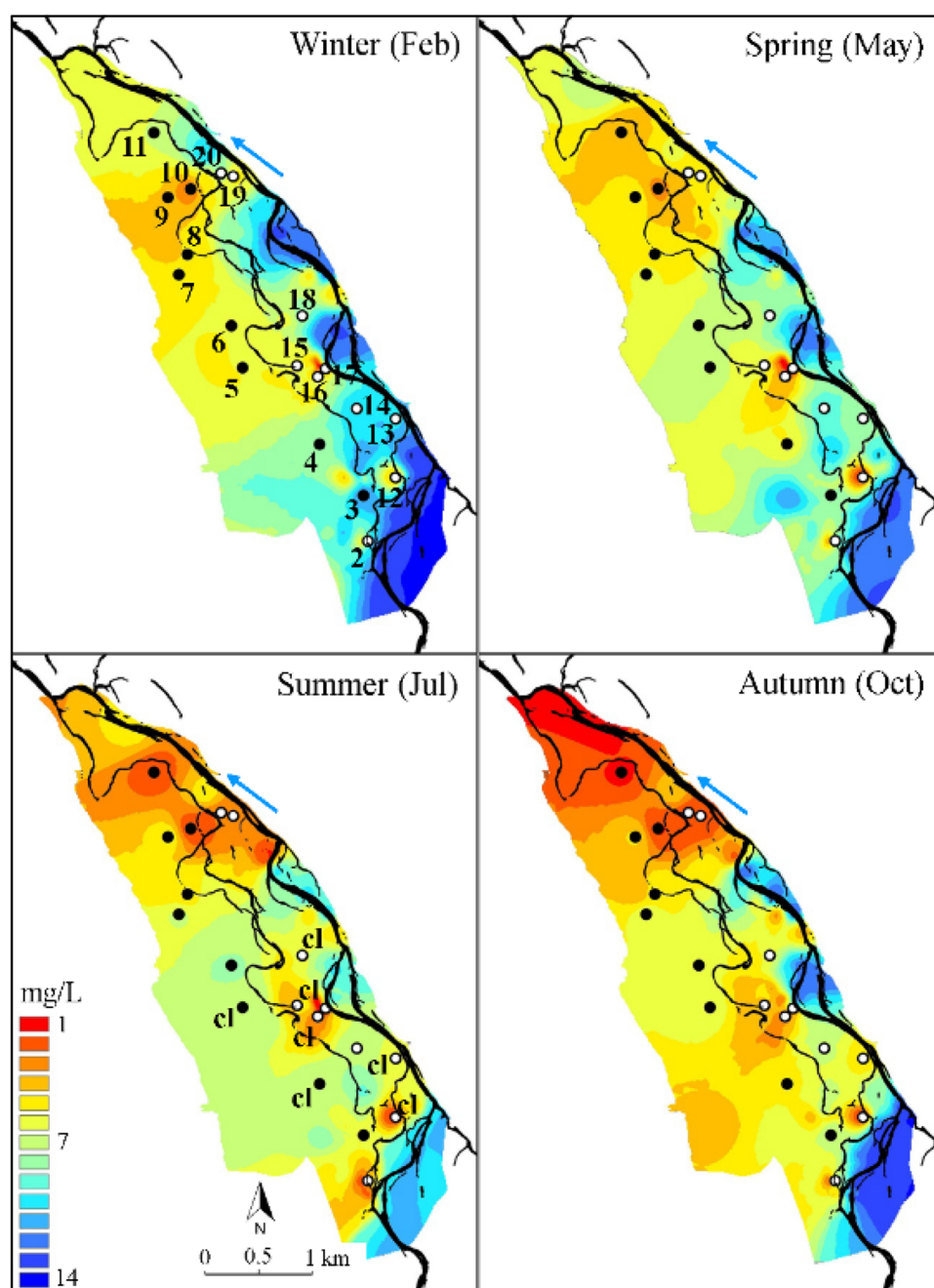


Figure 4. Seasonal patterns (2004) of groundwater DO concentrations (mg/L) at the Nyack floodplain, Middle Fork Flathead River, MT illustrate simultaneous influence of flow and local conditions. River flow (*black lines*) is from the southeast to the northwest (*blue arrow*). Response surfaces were generated from kriging of concentrations ($n = 57$ wells) measured at 1 m depth. Symbols are wells in the active (*open*) and passive (*filled*) orthofluvial zones. Well numbers are in the *upper left panel* and correspond to those in Table 1. *cl* wells are identified in the *lower left panel*.

value more than 60 times the annual rate of decline derived from our analyses of the PO zone, and similar to those reported for flowpaths of comparably short lengths (150–300 m) in gravel bars of rivers in Washington, USA (Vervier and Naiman 1992), Australia (Cooling and Boulton 1993), and France (Marmonier and Dole 1986). These studies emphasize that river-aquifer interaction occurring along the AO zone may contribute to local conditions on the Nyack that then appear as distinct chemical and functional patches at the scale of our investigation.

Patch structure is also evident along the aquifer's vertical axis. Vertical gradients in DO observed within *cl* wells of the Nyack floodplain are comparable to those reported for other alluvial aquifers including a shallow unconfined aquifer in the Konza prairie, Kansas, USA (Macpherson and Sophocleous 2004), the Chalk aquifer, Berkshire, United Kingdom (Schürch and Buckley 2002), and a sandy aquifer adjacent to Lake Huron, ON, Canada (Barbaro and others 1994). These studies report typical patterns of DO loss with depth. In contrast within the predominantly horizontal flow system

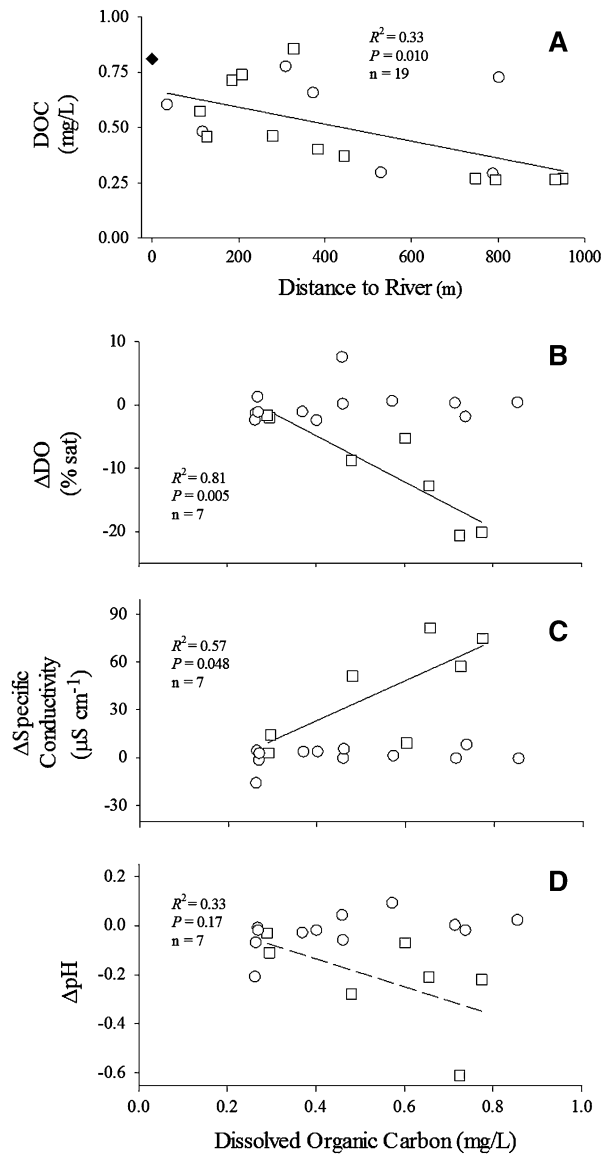


Figure 5. **A** DOC concentrations (mg/L) reflect distance from river channel (**A**) and are related to the extent of vertical organization in cl wells (**B–D**). Data are annual means for river (filled diamond, **A**), orthograde (open circles), and cl (open squares) wells. Solid lines depict significant ($P < 0.05$) regressions for all wells ($n = 19$, **A**) and for cl wells ($n = 7$, **B–D**). Dashed line in **D** indicates nonsignificant slope ($P > 0.05$). Mean DOC concentration for a given well was derived using average seasonal values ($n = 4$). Vertical differences in physicochemistry of cl wells were assessed using averages calculated from individual surveys of deep wells ($n = 5$, Appendix A in supplementary material).

of the Nyack floodplain, all cl wells were found in patches where DO minima occurred in shallow strata and concentrations increased with depth (Figure 2). Interestingly, two wells (PO4, Figure 2; AO16, data not shown) displayed strong vertical

gradients in all physicochemical variables, but little variation in temperature of deep (> 5 m) water compared to other cl wells. Temperature of groundwater in intermediate or regional flow systems is typically equivalent to average air temperature (Fetter 2001). For the two wells lacking temporal variation in deep groundwater, average temperature (6.9 and 7.9°C) corresponded closely to local mean air temperature at nearby Essex, MT (Western Regional Climate Center, www.wrcc.dri.edu). These are the only data suggesting influence by a stable groundwater source not heavily influenced by exchange with the river system.

Physicochemical patterns within and among wells of the Nyack floodplain suggest stoichiometric coupling driven by metabolic activity. Within cl wells, decreased DO at shallow depth was accompanied by decreased pH and increased ionic strength (Table 5) with no apparent relationship to sediment stratigraphy or variation in hydraulic conductivity (Appendix B in supplementary material). These patterns are consistent with aerobic oxygen consumption and concomitant acid and alkalinity production (Andrews and Schlesinger 2001; Smith and others 2011). Assuming an average alkalinity characteristic of the aquifer ($1,200 \mu\text{Eq L}^{-1}$, Reid 2007) and a respiratory quotient of 0.85 (Ellis and others 1998), changes in pH generated by aerobic respiration calculated using inorganic carbon equilibria (Smith and others 2011) represent about 35–50% of the observed decline in DO across four representative profiles in cl wells. The association between organic carbon abundance and the magnitude of vertical differences in DO, EC, and pH (Figure 5) also supports biotic origin of patch structure; greater DOC concentrations may fuel enhanced metabolic activity that corresponds to more abrupt gradients in DO and EC.

Not all patches of low DO, however, displayed evident vertical structure; three wells of lowest oxygen content (PO10, PO11, and AO20, Table 1) were found far down the floodplain, but were all orthograde. Although the next most hypoxic environments (AO12 and AO17) were characterized by cl profiles, they were near the head of the floodplain (Figure 1). Low DO found in wells at the head of the floodplain with evident vertical structure related to DOC supply argues that these wells were located in metabolic hot spots. With this distinction, the majority of hotspots (5 of 7) were located within the active portion of the orthofluvial zone, reflect smaller-scale, more local conditions, and their persistence must be tied to reliable sources of labile organic carbon (Battin and others 2003).

Transport and Metabolism: Implications for Local Versus Routing Control

Our study proposes that a combination of hydraulic routing and local metabolism results in the physicochemical structure observed in the Nyack's alluvial aquifer. Carbon supply to the Nyack aquifer may be derived from the river via hydrologic routing (Helton and others 2012) as DOC (Ellis and others 1998; Reid 2007). We observed declines in DOC concentration with increasing distance from the river (Figure 5) consistent with the argument for riverine sourcing of organic carbon. These gradients were most evident during summer when longitudinal organization was weakest and DO heterogeneity greatest (Figure 4, Appendix C in supplementary material).

Particulate sources of organic matter may also contribute to subsurface metabolism and groundwater biogeochemical structure (Pusch and Schworerbel 1994; Crenshaw and others 2002). Brugger and others (2001), however, emphasized that particulates were effectively filtered from groundwater flowpaths at the surface–subsurface interface of a riparian aquifer. Given the spatial scales applicable to the Nyack's flowpaths, it is likely that the influence of river-derived fine particulate organic matter is restricted to parafluvial zones near the river's main channel.

Entrainment during large floods may result in the deposition and burial of wood that may fuel microbial metabolism (Guyette and Stambaugh 2003; Guyette and others 2008). Patch origin and composition of this type would generate hot spots distributed across active and PO zones associated with changes in channel location (Whited and others 2007), patterns congruent with those observed in our study. Further, buried wood would serve as a carbon source that would persist over the long periods of time required to be evident across seasons. Although deposits of this type have been noted in exposed banks on the floodplain (Stanford, pers. obs.), little is known about the capacity for buried wood to fuel metabolic activity in the Nyack aquifer.

Finally, vertical infiltration and groundwater recharge through the soils of the floodplain itself may serve as a carbon source fueling subsurface processes that generate biogeochemical structure (Baker and others 2000). Delivery of DOC from overlying soils would explain the observed vertical zonation, especially if water table elevations inundate soil horizons during high water conditions (Appendix B in supplementary material). Six of seven wells displaying cl profiles occurred in “ma-

ture forest” plots whose composition had not changed greatly over a 60-year monitoring period (Whited and others 2007), but soil depths varied widely among wells without relation to the degree of vertical zonation. At the same time, wells with the lowest DO (for example, PO10) were often orthograde in character and retained their vertical profiles throughout all seasons. In contrast, carbon inputs from soil horizons would most likely be limited to shorter time frames associated with leaching following precipitation events (Harms and Grimm 2008) or seasonal elevation of the water table (Baker and others 2000).

CONCLUSIONS

Spatial and temporal variation in the physicochemical characteristics of the Nyack aquifer reflects local and routing organization that is likely a general feature of all floodplain landscapes. Routing control results from the predominant influence of the flow of water down-gradient and the linkages provided by the directional character of rivers and their interaction with floodplain ecosystems (Junk and others 1989; Noe and Hupp 2005). At the same time, physical discontinuities (Poole 2002), patchiness in resource availability (Pringle and others 1988), and advective fluxes at smaller scales (Poole and others 2004) emphasize local influences on form and function.

Across time, seasonal change shifts the relative influences of routing control when longitudinal decline in DO and associated physicochemical conditions reflect metabolic processing along flowpaths typical of transport-dominated systems (Fisher and others 2004), and local control when ambient supplies of energy and materials interact to generate distinct patches. A similar distribution from routing to local control occurs across space. Within the PO zone, longitudinal flowpaths organize physicochemical structure over all time scales, whereas the AO zone is always characterized by heterogeneous physicochemical patches.

Sponseller and Fisher (2008) emphasized shifts from routing to local control across spatial scales in a desert landscape where distinction among patches was relevant at one scale, but overcome by routing influences at another. We contend that the interplay between routing and local control is characteristic of all landscapes (Seastedt and others 2004) and further research into their relative influence on form and function will contribute to an emerging science of spatial ecosystem ecology (Turner 1989).

ACKNOWLEDGMENTS

Major funding and material support was provided by National Science Foundation (NSF) Grant EAR-0120523 to JAS, and DDIG (NSF 02-173) to FRH and BLR. Thanks to Curtis Monteau who was supported by NSF UMEB DEB-9975365. Support for HM Valett was provided to HMV by NSF EPSCoR Track-1 EPS-1101342 (INSTEP 3) through the MT Institute on Ecosystems and by NSF MCB-0348773 to JAS and NSF EPS-0701906 to FRH. Diane Whited provided the kriging analyses and graphics.

REFERENCES

- Andrews JA, Schlesinger WH. 2001. Soil CO₂ dynamics, acidification, and chemical weathering in a temperate forest with experimental CO₂ enrichment. *Glob Biogeochem Cycles* 45:149–62.
- Baker MA, Valett HM, Dahm CN. 2000. Organic carbon supply and metabolism in a shallow groundwater ecosystem. *Ecology* 81:3133–48.
- Barbaro SE, Albrechtsen HJ, Jensen BK, Mayfield CI, Barker JF. 1994. Relationships between aquifer properties and microbial populations in the borden aquifer. *Geomicrobiol J* 12:203–19.
- Battin TJ, Kaplan LA, Newbold JD, Hendricks SP. 2003. A mixing model analysis of stream solute dynamics and the contribution of a hyporheic zone to ecosystem function. *Freshw Biol* 48:995–1014.
- Brugger A, Reitner B, Kolar I, Queric N, Herndl GJ. 2001. Seasonal and spatial distribution of dissolved and particulate organic carbon and bacteria in the bank of an impounding reservoir on the Enns River, Austria. *Freshw Biol* 46:997–1016.
- Butler JJ, Garnett EJ, Healey JM. 2003. Analysis of slug tests in formations of high hydraulic conductivity. *Groundwater* 41:620–31.
- Connell JH, Slatyer RO. 1977. Mechanisms of succession in natural communities and their role in community stability and organization. *Am Nat* 111:1119–44.
- Cooling MP, Boulton AJ. 1993. Aspects of the hyporheic zone below the terminus of a south Australian arid-zone stream. *Aust J Mar Freshw Res* 44:411–26.
- Craft JA, Stanford JA, Pusch M. 2002. Microbial respiration within a floodplain aquifer of a large gravel-bed river. *Freshw Biol* 47:251–61.
- Crenshaw CL, Valett HM, Webster JR. 2002. Effects of augmentation of coarse particulate organic matter on metabolism and nutrient retention in hyporheic sediments. *Freshw Biol* 47:1820–31.
- Diehl JC. 2004. Hydrogeological characteristics and groundwater/river exchange in a gravel-dominated floodplain, Middle Fork of the Flathead River, Northwestern Montana. Master's Thesis, The University of Montana, 168 p.
- Dimond WJ, Armstrong DP. 2007. Adaptive harvesting of source populations for translocation: a case study with New Zealand Robins. *Conserv Biol* 21:114–24.
- Ellis BK, Stanford JA, Ward JV. 1998. Microbial assemblages and production in alluvial aquifers of the Flathead River, Montana. *J N Am Benthol Soc* 17:382–402.
- ESRI. 2010. ArcGIS ArcMap, Version 10. Redlands, CA: Esri.
- Fetter CW Jr. 2001. Applied hydrogeology. 4th edn. Lebanon: Prentice Hall. p 598.
- Fisher SG, Likens GE. 1973. Energy flow in Bear Brook, New Hampshire: an integrative approach to stream ecosystem metabolism. *Ecol Monogr* 43:421–39.
- Fisher SG, Sponseller RA, Heffernan JB. 2004. Horizons in stream biogeochemistry: flowpaths to progress. *Ecology* 85:2369–79.
- Guyette RP, Stambaugh MC. 2003. The age and density of ancient and modern oak wood in streams and sediments. *IAWA J* 24(4):345–53.
- Guyette RP, Dey DC, Stambaugh MC. 2008. The temporal distribution and carbon storage of large oak wood in streams and floodplains. *Ecosystems* 11:643–53.
- Hanski I. 1998. Metapopulation dynamics. *Nature* 396:41–9.
- Harms TK, Grimm NB. 2008. Hot spots and hot moments of carbon and nitrogen dynamics in a semiarid riparian zone. *J Geophys Res Biogeosci* 113:G01020.
- Harvey JW, Bencala KE. 1993. The effect of streambed topography on surface–subsurface water exchange in mountain catchments. *Water Resour Res* 29:89–98.
- Heffernan J, Sponseller R, Fisher SG. 2008. Consequences of a biogeomorphic regime shift for the hyporheic zone of a Sonoran Desert stream. *Freshw Biol* 53:1954–68.
- Helton AM, Poole GC, Payn RA, Izurieta C, Stanford JA. 2012. Relative influences of the river channel, floodplain surface, and alluvial aquifer on simulated hydrologic residence time in a montane floodplain. *Geomorphology*. doi:10.1016/j.geomorph.2012.01.004.
- Hopkinson CS, Buffam I, Hobbie J, Vallino J, Perdue M, Eversmeyer B, Prahl F, Covert J, Hodson R, Moran MA, Smith E, Baross J, Crump B, Findlay S, Foreman K. 1998. Terrestrial inputs of organic matter to coastal ecosystems: an intercomparison of chemical characteristics and bioavailability. *Biogeochemistry* 43:211–34.
- Howarth R, Schneider R, Swaney D. 1996. Metabolism and organic carbon fluxes in the tidal freshwater Hudson River. *Estuaries* 19:848–65.
- Hutchinson GE. 1961. The paradox of the plankton. *Am Nat* 95:137–45.
- Jansson M, Bergstrom AK, Blomquist P, Drakare S. 2000. Allochthonous organic carbon and phytoplankton/bacterioplankton production relationships in lakes. *Ecology* 81:3250–5.
- Junk WJ, Bayley PB, Sparks RE. 1989. The flood pulse concept in river-floodplain systems. *Can Spec Pub Fish Aquat Sci* 106:110–27.
- Leibold MA, Holyoak M, Mouquet N, Amaresekare P, Chase JM, Hoopes JM, Holt RD, Shurin JB, Law R, Tilman D, Loreau M, Gonzalez A. 2004. The metacommunity concept: a framework for multi-scale community ecology. *Ecol Lett* 7:601–13.
- Levine JM. 2000. Species diversity and biological invasions: relating local process to community pattern. *Science* 288:852–4.
- Loreau M, Mouquet N, Holt RD. 2003. Meta-ecosystems: a theoretical framework for a spatial ecosystem ecology. *Ecol Lett* 6:673–9.
- Macpherson GL, Sophocleous M. 2004. Fast ground-water mixing and basal recharge in an unconfined, alluvial aquifer, Konza LTER site, northeastern Kansas. *J Hydrol* 286:271–99.
- Malard F, Hervant F. 1999. Oxygen supply and the adaptations of animals in groundwater. *Freshw Biol* 41:1–30.

- Marmonier P, Dole MJ. 1986. Les amphipodes des sédiments d'un bras court-circuité du Rhone. *Sci de L'Eau* 5:461–86.
- Minshall GW. 1967. Role of Allochthonous Detritus in the trophic structure of a Woodland Springbrook Community. *Ecology* 48:139–49.
- Montgomery DR. 1999. Process domains and the river continuum. *J Am Water Resour As* 35:397–410.
- Mulholland PM, Newbold JD, Elwood JW, Ferren LA, Webster JR. 1985. Phosphorus spiraling in a woodland stream: seasonal variations. *Ecology* 66:1012–23.
- Noe GB, Hupp CR. 2005. Carbon, nitrogen, and phosphorus accumulation in floodplains of Atlantic coastal plain rivers, USA. *Ecol Appl* 15:1178–90.
- Odum HT. 1956. Primary production in flowing waters. *Limnol Oceanogr* 1:102–17.
- Odum EP, de la Cruz AA. 1963. Detritus as a major component of *ecosystems*. *AIBS Bull.* 13:39–40.
- Pace ML, Cole JJ, Carpenter SR, Kitchell JF, Hodgson JR, Van de Bogert MC, Bade DL, Kritzberg ES, Bastviken D. 2004. Whole-lake carbon-13 additions reveal terrestrial support of aquatic food webs. *Nature* 427:240–3.
- Pepin DM, Hauer FR. 2002. Benthic responses to groundwater–surface water exchange in an alluvial river. *J N Am Benthol Soc* 21:370–83.
- Polis GA, Power ME, Huxel GR, Eds. 2004. *Food webs at the landscape level*. Chicago, IL: University of Chicago Press.
- Poole GC. 2002. Fluvial landscape ecology: addressing uniqueness within the river discontinuum. *Freshw Ecol* 47:641–60.
- Poole GC, Stanford JA, Running SW, Frissell CA, Woessner WW, Ellis BK. 2004. A patch hierarchy approach to modeling surface and subsurface hydrology in complex flood-plain environments. *Earth Surf Proc Land* 29:1259–74.
- Pringle CM, Naiman RJ, Bretschko G, Karr JR, Oswood MW, Webster JR, Welcomme RL, Winterbourn MJ. 1988. Patch dynamics in lotic systems: the stream as a mosaic. *J N Am Benthol Soc* 7:503–24.
- Pusch M, Schwoerbel J. 1994. Community respiration in hyporheic sediments of a mountain stream (Steina, Black Forest). *Arch Hydrobiol* 130:35–52.
- Pusch M, Fiebig D, Brettar I, Eisenmann H, Ellis BK, Kaplan LA, Lock MA, Naegeli MW, Traunspurger W. 1998. The role of micro-organisms in the ecological connectivity of running waters. *Freshw Biol* 40:453–95.
- Reid BL. 2007. Energy flow in a floodplain aquifer ecosystem, PhD Thesis. Missoula, MT: The University of Montana.
- Ricklefs RE. 1987. Community diversity: relative roles of local and regional processes. *Science* 235:167–71.
- Schlesinger WH, Raikes JA, Hartley AE, Cross AF. 1996. On the spatial pattern of soil nutrients in desert ecosystems. *Ecology* 77:364–74.
- Schürch M, Buckley D. 2002. Integrating geophysical and hydrochemical borehole-log measurements to characterize the Chalk aquifer, Berkshire, United Kingdom. *Hydrogeol J* 10:271–99.
- Seastedt TR, Bowman WD, Townsend A, Williams MW, Caine TN, McKnight DM. 2004. The landscape continuum: a model for high-elevation ecosystems. *Bioscience* 54:111–24.
- Smith GM, Parker SR, Gammons CH, Poulson SR, Hauer FR. 2011. Tracing dissolved oxygen and dissolved inorganic carbon stable isotope dynamics in the Nyack aquifer: Middle Fork Flathead River, Montana, USA. *Geochim Cosmochim Acta* 75:5971–86.
- Sponseller R, Fisher SG. 2008. The influence of drainage networks on patterns of soil respiration in a desert catchment. *Ecology* 89:1089–100.
- Stanford JA, Ward JV. 1988. The hyporheic habitat of river ecosystems. *Nature* 335:64–6.
- Stanford JA, Lorang MS, Hauer FR. 2005. The shifting habitat mosaic of river ecosystems. *Verh Internat Verein Limnol* 29:123–36.
- Turner MG. 1989. Landscape ecology: the effect of pattern on process. *Annu Rev Ecol Syst* 20:171–97.
- Vannote RL, Minshall GW, Cummins KW, Sedell JR, Cushing CE. 1980. The river continuum concept. *Can J Fish Aquat Sci* 37:130–7.
- Vervier P, Naiman RJ. 1992. Spatial and temporal fluctuations of dissolved organic carbon in subsurface flow of the Stillaguamish River. *Arch Hydrobiol* 123:401–12.
- Whited DC, Lorang MS, Harner MJ, Hauer FR, Kimball JS, Stanford JA. 2007. Climate, hydrologic disturbance, and succession: drivers of floodplain pattern. *Ecology* 88:940–53.
- Wyatt KH, Hauer FR, Pessoney GF. 2008. Benthic algal responses to hyporheic–surface water exchange in an alluvial river. *Hydrobiologia* 607:151–62.